

# Response Analysis of Yokohama Bay Bridge under the 2011 Great East-Japan Earthquake

**D.M. Siringoringo & Y. Fujino**

*Bridge & Structure Laboratory, Dept. of Civil Eng., Univ. of Tokyo*



## **SUMMARY:**

Yokohama Bay Bridge with the total span length of 860m is the second longest span cable-stayed bridge in the eastern part of Japan and one of the most densely instrumented bridges in Japan. On March 11, 2011, northeastern Japan was shaken by the Great East-Japan earthquake and the JMA seismic intensity 5+ (upper 5) out of the maximum scale of 7 was recorded at the bridge location. This paper describes analysis of the bridge seismic response recorded by monitoring system focusing on the following subjects: 1) temporal and spectral analysis of the bridge responses, 2) system identification and observation of the changes in modal parameters with respect to earthquake amplitude, 3) performance evaluation of link-bearing connection –a seismic isolation device, during the earthquake and 4) post-earthquake field observation.

*Keywords: seismic record analysis, cable-stayed bridge, Great East Japan earthquake*

## **1. INTRODUCTION**

Yokohama-Bay Bridge is a part of the Tokyo-Yokohama Bay Shore expressway link that connects Tokyo and Yokohama harbor area. The bridge is a continuous three-span cable-stayed with the total span length of 860m consisting of 460m center span and 200m side spans (Figure 1). The main girder consists of double-deck steel truss-box: six lanes upper deck and two lanes lower deck. The bridge has two H-shaped towers welded as monolithic section with the height of 172m and width of 29.25m. Earthquake resistance is one of the main concerns in the bridge design. Considering seismic history of the area and the possible recurrence of large earthquake such as the 1923 Great Kanto earthquake, the weak ground and high location of the bridge's center of gravity, the bridge adopted a special seismic design measure. Using this measure, the girder is suspended from towers and piers by means of link bearing connections (LBC) in such a way that the effect of superstructure inertia force on the substructure is reduced during an earthquake by maintaining a longitudinal fundamental period of about 7.7sec. As a result, during an earthquake, the girder is expected to have lower acceleration but larger displacement (Yokohama Bay Bridge 1991).

The bridge has undergone seismic retrofit in 2005, where safety assurance for level 2 ground motions in Japanese seismic code was of primary concern. Two types of the maximum credible earthquakes were considered in the retrofit program. They were type-I ground motion (far-field or moderately far-field large earthquake taking place in the subduction zone of the Pacific plate) with a magnitude of order 8 and type-II ground motion (near field ground motion due to inland earthquake occurring beneath the site or close to the site) (Fujino et al. 2005). To monitor dynamic response and seismic performance, a monitoring system consisting of eighty-five sensors measuring acceleration and displacement at 36 locations was installed on the bridge. Along the girder, sensors are installed at 12 locations with spacing of 115 m (Figure 1). Bridge responses were collected by controller every time accelerations exceed the preset trigger level. The monitoring system is operated by Tokyo Metropolitan Expressway Public Corporation.

At 14:46 Japan Standard Time (JST) on March 11, 2011, the northeastern Japan was struck by the Great East Japan earthquake with moment magnitude of 9.0. Epicenter of the earthquake was about 398km away from the bridge, with the focal depth of 24km. Even though the epicenter is very far away from the bridge, the entire fault rupture consists of 500km long from north to south and 200km wide area off the coast of northeast Japan. This means that the closest distance from the bridge to the rupture fault area is about 180km. JMA seismic intensity 5+ (equivalent to scale VII in MMI), out of maximum 7 was recorded on the bridge location.

This paper describes response analysis of Yokohama Bay Bridge under 2011 Great East Japan earthquake. The study describes response analysis of the main shock event on March 11, 2011 and several aftershocks with the JMA seismic intensity equal to or larger than 3. The high-quality seismic responses recorded on the bridge is significant considering that the earthquake magnitude and seismic intensity on bridge site is one of the largest ever recorded on a completed long-span cable-stayed bridge in Japan, and the number of vibration sensors used in the bridge is larger than those used in any other instrumented cable-stayed bridges in Japan. The paper emphasizes on the seismic response of superstructure, with the following subjects: 1) temporal and spectral analysis of the bridge responses, 2) system identification and observation of the changes in modal parameters with respect to earthquake amplitude, 3) performance evaluation of LBC during the earthquake and 4) post-earthquake visual inspection.

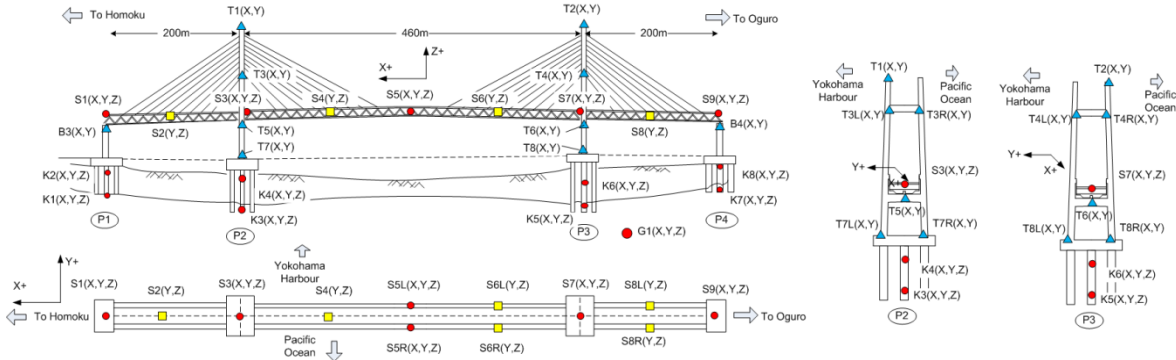


Figure 1. Yokohama-Bay Bridge’s sensor arrangement for seismic monitoring system

2. CHARACTERISTICS OF RECORDED SEISMIC RESPONSES

The input excitations recorded on the bridge foundation are still below the design and seismic-retrofit ground motions. The bridge experienced intense shaking for about 10 minutes but no structural damage was reported.

2.1. Characteristics of Recorded Girder Responses

The bridge superstructure responses were characterized by large transverse vibration (Table 1). The girder maximum acceleration was recorded in transverse direction, with the maximum girder displacement of more than 60cm recorded in the middle of center-span. The girder large vibration is mainly due to one mode that is the first girder transverse mode at 0.28-0.32Hz. Meanwhile, the girder vertical vibration is dominated by the first five vertical bending modes between 0.32Hz and 1.2Hz. The maximum girder vertical displacement is about 20cm measured at the middle of the center span. Frequency characteristics during main shock suggest that the predominant girder frequencies are closely-spaced around 0.32Hz for both vertical and transverse directions. The results differ from the previous estimation under smaller earthquakes (Siringoringo and Fujino 2006), where the first vertical and transverse mode was identified at 0.34Hz and 0.28Hz, respectively. Considering that bridge responses may enter non-linear region at large excitation, frequency spectra of the overall responses may not be adequate to represent time variation of the natural frequencies. Therefore, a time-frequency

analysis by wavelet transform was conducted. The scalogram of transverse acceleration shows frequency peak at the initial response appears at 0.29Hz (Figure 2). The frequency increases and reaches up to 0.32Hz during the largest excitation (i.e.100-200sec) before later decreases to 0.27Hz near the end of response. On contrary for the vertical acceleration, the frequency peak at the initial response appears at 0.34Hz. The frequency decreases slightly to 0.32Hz during the largest excitation, but increases to 0.34Hz near the end of the response. The similar result was also observed during aftershock 1 (March 11, 2011 15:16). Changes in transverse and vertical frequencies indicate non-linearity of the response. However, it should be mentioned that girder accelerations are subjected to the conditions of ground motions. Therefore to have a complete understanding of the change in modal parameters, a system identification technique should be utilized, which will be explained further in this paper.

**Table 1.** Recorded accelerations and displacements during the main shock (March 11, 2011 14:47)

Sensor Code and Location	Max Acceleration [direction] (cm/s <sup>2</sup> )	Max Displacement (cm)
S5 R (Girder, mid of center-span)	51.14 [L], 299.17 [T], 194.25 [V]	19.60 [L], 61.80 [T], 19.50[V]
S4 (Girder, quarter of main span )	250.78 [T], 163.58 [V]	47.15 [T], 11.32 [V]
S2 (Girder, midpoint of side span )	335.77 [T], 165.80 [V]	20.50 [T], 6.94 [V]
T1 (Top of tower P2)	252.99 [O], 635.94 [I]	25.00 [O], 54.60 [I]
T2 Top of tower P3	418.67 [O], 656.87 [I]	24.28 [O], 48.36 [I]
T3 (Middle of tower P2)	124.37 [L], 344.41 [T]	23.40 [L], 43.40 [T]
T4 (Middle of tower P3)	138.80 [L], 411.73 [T]	22.50 [L], 42.70 [T]
T8 (Bottom of tower, footing slab)	71.38 [L], 67.27 [T]	17.50 [L] , 18.00 [T]

Note: L= Longitudinal, T= Transverse, V= Vertical, O=out-of-plane, I= in-plane

## 2.2. Characteristics of Recorded Tower Responses

Maximum acceleration larger than 600 cm/s<sup>2</sup> was recorded on the top of both towers giving the maximum tower in-plane displacement of more than 50cm. The large tower in-plane vibrations were mainly dominated by the modes that correspond to the tower local frequency at 0.42Hz. In the out-of-plane direction, the maximum accelerations were 252 cm/s<sup>2</sup> and 418 cm/s<sup>2</sup> for P2 and P3, respectively. The tower out-of-plane vibrations were mainly due to the bridge global modes associated with girder vertical modes such as the first vertical bending (0.32Hz-0.34Hz) and the first torsional mode (0.83Hz), with the largest component is due to the second vertical bending modes at around 0.50Hz.

## 2.3. Characteristics of Vibration on Pier-to-Girder and Tower-to-Girder Connections

Girder motion in longitudinal direction is accommodated by link-bearing connections (LBC), namely, end-link at the end of girder (P1 and P4) and tower-link at the towers (P2 and P3). The LBC is a double head pendulum with the length of 10m and 2 m, for the end-link and the tower-link, respectively. The upper and lower head connect the end-link to girder and pier, respectively. Meanwhile, it is the opposite condition for the tower-link (Figure 3). Each of pendulum head is made of steel discs and connected by bolts on its circumference.

In transverse direction, the girder movement is restricted by wind shoes at all piers and towers. Small transverse gap exists between wind shoe and girder to allow for tower-girder transverse relative motion. Surface of the wind shoes are made of stainless steel. Meanwhile side bearings are installed on girder connection's side that faces the wind shoe. The side bearings on the girder-to-end pier and girder-to-tower connections have concave surface made of Teflon PTEE and are designed for transverse load of 2,820ton and 4,930ton, respectively.

In design, the LBCs are expected to slide during an earthquake so that large vibration energy from the pier or tower would not be transferred to the girder and vice-versa (Maeda et al. 1991). In such condition, relative displacement between pier and girder; and between tower and girder will be sufficiently large and the high frequency components of the pier and tower vibration will not be transferred to girder. Figure 4 shows that pier longitudinal acceleration (B3X) was dominated by

frequency peaks around 1.5Hz and 2Hz, while the girder longitudinal acceleration (S1X) located on the top of B3X was dominated by frequency peaks around 0.13Hz. Spectra plots of accelerations show that vibration energy at the girder is significantly smaller compared to that of the pier. The maximum acceleration on the pier is about  $500\text{ cm/s}^2$  while the maximum acceleration at the girder is only about  $50\text{ cm/s}^2$ . The facts that girder longitudinal acceleration is dominated by low frequency component, significant reduction in high frequency components of girder longitudinal acceleration and the large difference of vibration amplitude between pier and girder indicate that vibration energy from the pier was not transferred to the girder. Similar results were also observed on longitudinal responses of tower at the deck level (T5X and T6X).

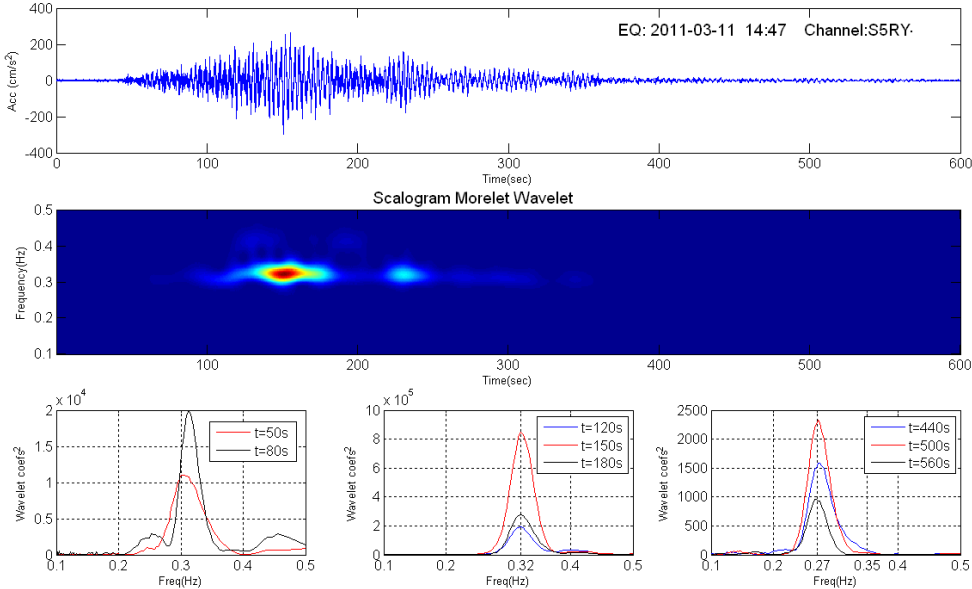


**Figure 2.** Scalogram of girder transverse acceleration during main shock and its ridges for several time stamps

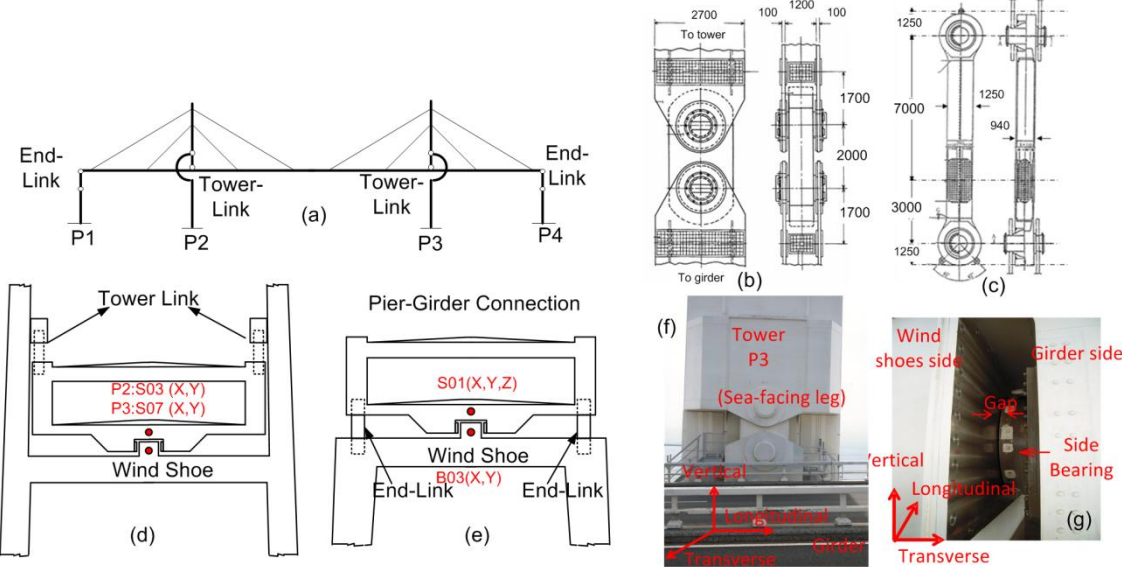


**Figure 3.** (a) Characteristics of pier-to-girder and tower-to-girder connections, (b) detail figure of tower-link, (c) detail figure of end-link, (d) Schematic figure of tower-to-girder connection, (e) Schematic figure of pier-to-girder connection, (f) photo of tower link and (g) snapshot photo of wind shoe transverse gap between tower/pier and girder.

Girder longitudinal displacement is one of the main concerns in design. Excessive longitudinal displacement during a large earthquake may cause pounding to the approach spans and result in

damage to the pier-to-girder connections. The seismic records show, however, that the girder maximum longitudinal displacement (processed from acceleration) was relatively small, in the order of 20cm and is far below the maximum allowable displacement 1.5m anticipated in the seismic retrofit program. Relative displacement between girder and tower or between girder and piers at connections can be used as indicators of pier-to-girder and tower-to-girder performance during earthquakes. The results show that relative displacement between pier and girder in longitudinal direction are in order of 5-10cm (Figure 5). In fact at P1, pier-cap displacement (B3X) was lagged behind the girder (S1X) displacement during the largest excitation (time: 150-200sec) suggesting that girder movement was completely decoupled from pier movement for that short period of time. Meanwhile relative longitudinal displacements between girder and tower at connection are smaller than that of pier (1-5cm).

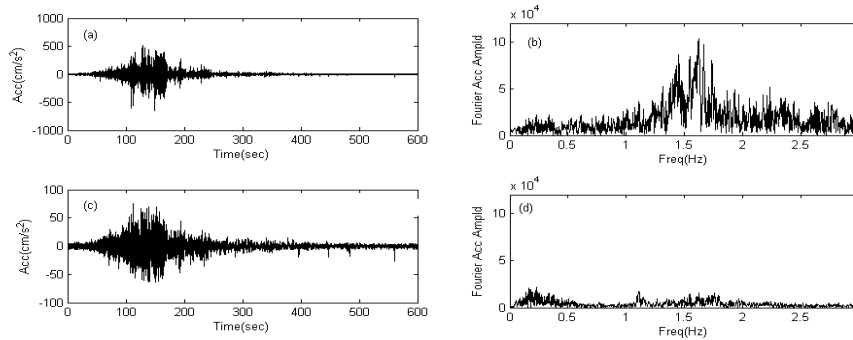


**Figure 4.** (a) Longitudinal acceleration recorded on pier P1 (B3X), (b) Fourier spectrum of acceleration B3X, (c) Longitudinal acceleration recorded on the girder above P1 pier (S1X) (d) Fourier spectrum of acceleration S1X

Figure 6 shows a close-up look of the acceleration response recorded by sensors T5Y on the wind shoes during the main shock, where one can see clearly periodic impulse indicating the occurrence of transverse pounding between tower and girder. Similar periodic impulses are also observed during the largest aftershock (i.e. March 11 15:16 JST). By observing time intervals between successive impulses during the largest excitation, we can estimate the structural mode corresponding to the motion when pounding occurs. The average time interval between consecutive impulses is about 3.2 second that corresponds to periodic motion with frequency about 0.32Hz. This result indicates that the transverse impulse at the tower-to-girder during the largest excitation period of the main shock was mainly caused by the girder first transverse mode.

### 3. SYSTEM IDENTIFICATION

Multiple-input multiple output (MIMO) system identification was employed to identify modal parameters of the bridge under seismic excitation. The methodology used in this study utilizes correlations between input-output data for realization of a state-space model and estimation of modal parameters (Siringoringo and Fujino 2008). To implement the system identification, a set of input-output data was selected. Inputs are responses from triaxial accelerometers located at the bottom of the towers (P2 and P3) and the end-pier (P1). While outputs are 41 channels of acceleration from super structures consisting of girder (23 channels), pier P1 (2 channels), tower P2 (8 channels) and tower P3 (8 channels). Since the input and output data are from multiaxial accelerations, the identified mode shapes will have three-dimensional shape.

The system identification is based on assumption that modal parameters remain constant within the specific time-window in which the input-output data was analyzed. However, since the input excitation is large and the response is quite long, the bridge may enter non-linear region and the assumption may not always be satisfied. Therefore, the analysis was conducted on a shorter time frame in a moving time-window scheme. Assuming constant modal parameters is considered more

reasonable within this shorter time frame. For this reason, the total response of main shock was divided into twelve time frames consisting of 50 seconds of input and output data (i.e. frame 1,2,...12) that each generates a set of modal parameters. The same procedure was also applied to aftershock responses.

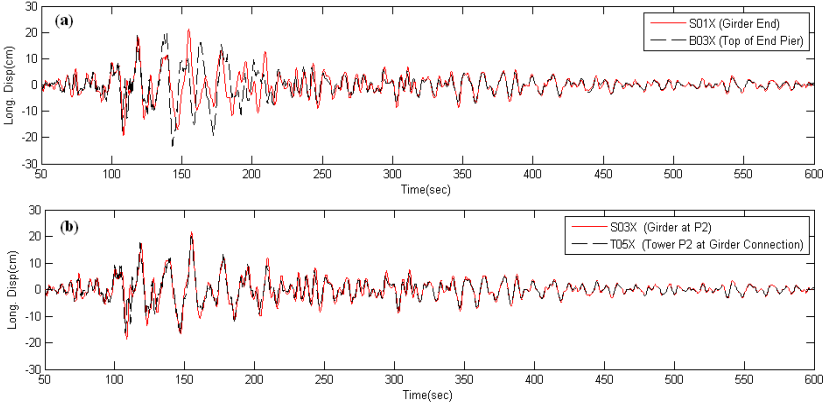


Figure 5. Comparison of longitudinal displacement (a) at end-pier P1 (B3X-S1X), (b) at tower P2 (S3X-T5X)

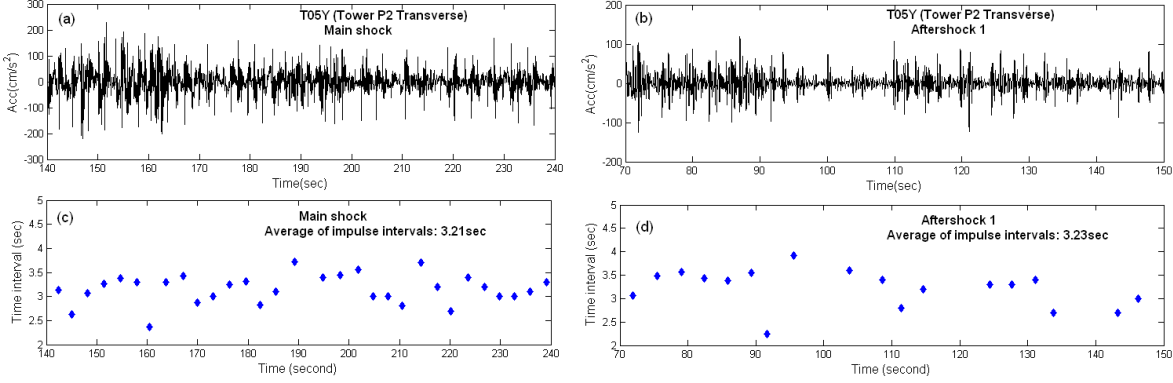


Figure 6. Accelerations of tower at deck level showing spike indicating impulses: (a) main shock (b) aftershock 15:16. Time interval of successive pulse responses (c) main shock (d) aftershock 15:16.

3.1. Results of system identification: longitudinal mode

System identification generated fourteen modes between 0.1Hz and 2.5Hz where the girder modal displacement dominates the mode shapes. Table 2 shows that the identified natural frequencies were in good agreement with the results from the previous earthquakes and the finite element model. The first three modes, namely, the girder first longitudinal, first transverse and first vertical mode dominate the girder vibration in three respective directions and are most sensitive to the input amplitude.

The first mode is the longitudinal sway mode characterized by dominant girder longitudinal modal displacement with minimum coupling in other directions. Shape and natural frequency characteristics of this mode depend on the behavior of LBC during vibration. In design, the LBC is modeled as a longitudinal hinge connection denoted as *slip mode*. Previous observations from seismic response of various level of earthquakes reveal that this is not necessary true (Siringoringo and Fujino 2006). For small earthquakes, system identification identifies the longitudinal mode shape with small relative modal displacements between end-piers and girder and higher frequency of longitudinal mode, denoted as *stick mode*. The *stick mode* suggests that LBC has not functioned as fully hinged connections and as a result force distribution on the end-piers and tower may be different than intended in design. Significant amount of additional moment will be redistributed to the bottom of pier

and tower if the LBCs remain stuck during large earthquake. Therefore it is important to investigate performance of LBC during large earthquake.

**Table 2.** Identified modal parameters from the main shock (March 11, 2011 14:47)

Mode	Freq (Hz)	Damp (%)	FEM (Hz)	Mode shape characteristics
Longtd (1)	0.14	7.76	0.14	Longitudinal swing mode (sliding)
Vertical (1)	0.33	4.20	0.34	Vertical 1st bending (1st Sym), small lateral coupling
(2)	0.51	1.21	0.49	Vertical 2nd bending (1st Asym) , no lateral coupling
(3)	0.75	3.49	0.77	Vertical 3rd bending (2nd Sym), no lat coupling
(4)	0.94	0.84	1.01	Vertical 4th bending (2nd Asym), small lateral coupling
(5)	1.10	1.34	1.21	Vertical 5th bending (3rd Sym) no lateral coupling
Torsion (1)	0.83	0.59	0.86	1st Torsion
(2)	1.41	2.59	1.38	2nd Torsion
(3)	2.41	1.80	2.45	3rd Torsion
Transverse(1)	0.32	0.47	0.28	Girder lateral 1st sym. bending coupled with girder vertical
(2)	0.53	2.63	N.A	Tower in-plane (P2 and P3 out-of-phase) coupled with girder vert.
(3)	0.42	1.34	0.42	Tower in-plane (P2 and P3 in-phase) no girder vertical-lateral coupl.
(4)	0.57	1.16	N.A	End Pier (P1) in-plane coupled with girder
(5)	1.10	1.34	1.08	Girder lateral 2nd bending (1st asym.) with small vertical coupling

Figure 7 shows the mode shape of longitudinal mode identified from main shock, frame 4 (t=150-200 during the largest excitation) and the mode was identified at 0.13Hz. Results of identification for the entire main shock response show that the mode was identified at around 0.12Hz-0.13Hz with large relative modal displacement between pier and girder indicating the *slip mode*. This is in agreement with the result of displacement of girder and pier at the pier-to-girder connection that shows a large relative displacement. It is also supported by the frequency characteristics of girder and pier accelerations at the pier-to-girder connection.

### 3.2. Coupling of girder vertical and transverse mode

The second and the third identified global mode were the first transverse bending and the first vertical bending, respectively. The two modes have distinct characteristics in that their natural frequencies and modal displacements depend on the amplitude of input excitation. During a large excitation, such as the 100-200 seconds of the main shock, frequency of the first transverse mode increases from 0.27Hz to 0.32Hz, while frequency of the first vertical mode decreases from 0.35Hz to 0.33Hz. The change in frequency is followed by the change in mode shape characteristics especially the girder transverse-vertical coupling pattern. During large excitation, strong transverse-vertical coupling of girder modal displacement was observed in both transverse and vertical modes, in such that the vertical mode has significant modal displacement in transverse direction and vice versa (Figure 8). During smaller excitation, as in the beginning and near the end of response, the transverse-vertical coupling becomes weaker resulting in the pure vertical and transverse mode (Figure 9). To quantify the coupling degree, an index  $\eta$  is defined as:

$$\eta_{v,t} = |\phi_{v,t}| / (|\phi_v| + |\phi_t|) \quad (1)$$

where  $\phi$  denotes the modal displacement of girder at the middle of center-span (i.e. node S5R) while the subscript V and T denotes the vertical and transverse, respectively. Variations of natural frequency and coupling behavior of the first lateral and first vertical bending modes with respect to input amplitude for all records analyzed are shown in Figure 10.

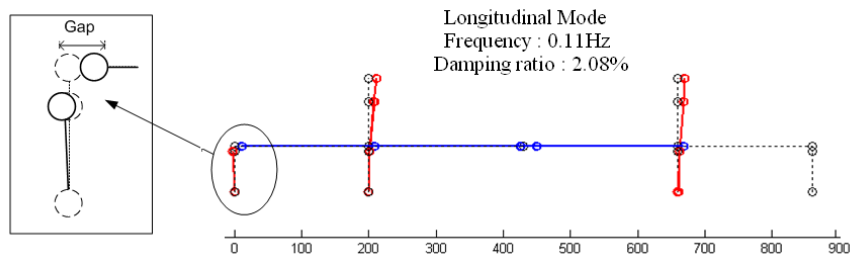


**Figure 7.** Longitudinal Mode shape with slip characteristic at the end-pier and girder connection

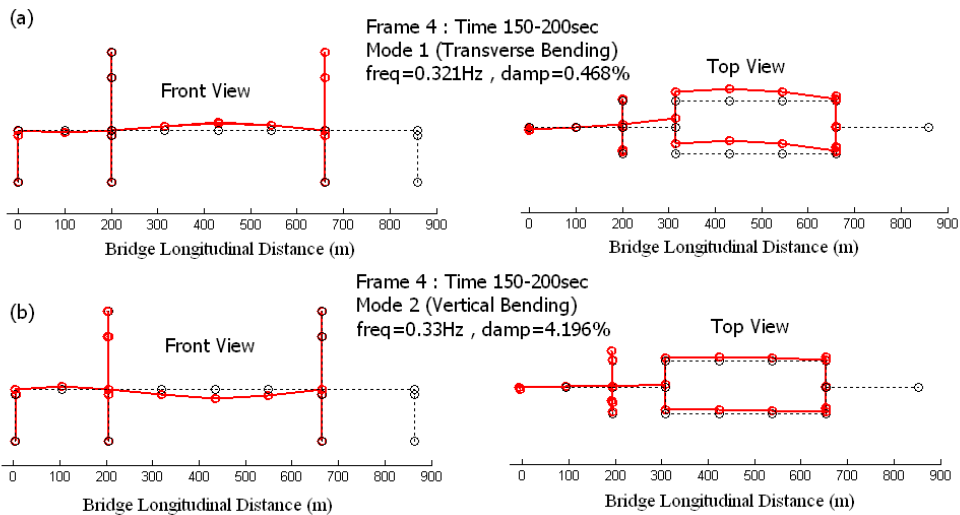


**Figure 8.** Characteristics of mode shapes with strong transverse-vertical coupling during the largest excitation of main shock 14:47 (Frame 4,  $t=150-200$ s): (a) girder first transverse mode and (b) girder first vertical mode.

The change in natural frequencies and the transverse-vertical coupling behavior with respect to input amplitude indicate that the bridge response has entered the non-linear region during the main shock. Several factors such as material nonlinearity, geometric nonlinearity due to large displacement in cable and behavior of pier-to-girder and tower-to-girder connections are known as the sources of non linearity in cable-stayed bridge seismic response. Considering that displacement resulted from seismic response is not so large as to cause significant geometric or material nonlinear, behavior of tower-to-girder and pier-to-girder connections are thought as a possible source of nonlinearity. Moreover, as mentioned previously, periodic impulse responses were observed on the acceleration records at both pier-to-girder and tower-to-girder connections. The impulse may be the result of transverse pounding between wind shoes and girder. The increase in natural frequency of the first transverse mode during large excitation indicates that the structure become stiffer in transverse direction.

#### 4. POST-EARTHQUAKE VISUAL INSPECTION

The bridge did not show any signs of serious structural damage and operation resumed following the earthquake. Visual inspection was conducted few times after the earthquake, and one of the objectives was to investigate condition of pier-to-girder and tower-to-girder connections. The results of visual inspection are as follows.

1. In longitudinal direction, circular marks was found on the surface of wind shoes of pier P1 and tower P2 suggesting that the girder had experienced large relative longitudinal movement. The marks show that relative displacement between girder and tower (and pier) in the order of 8-10cm had occurred (Figure 11(a)). For this relative displacement to occur, the link-bearing connection between girder and tower (and pier) must have slipped. This physical evidence supports the results of response analysis and the type of longitudinal mode generated by system identification. In

addition, since the wind shoe and girder is separated by small lateral gap, the mark left by girder on the wind shoe's side surface would only be possible if the wind shoes and girder jammed at some point in time during the excitation.

2. In transverse direction, several marks of scraped paint were observed on the link head of tower P2. Nuts of several bolts on the upper disc of the lower head of P2 tower link were crushed and signs of scraped paint can be clearly seen on the surface of the disc (Figure 11(c)). The scraped paint and broken nuts could be caused by transverse pounding between tower and girder at tower link and by combination of transverse and excessive vertical motion of girder at tower-to-girder connection. These physical evidences show that girder and tower have experienced large transverse vibration and may explain the occurrence of periodic impulses on the accelerations recorded by sensors near the pier-to-girder and the tower-to-girder connections.

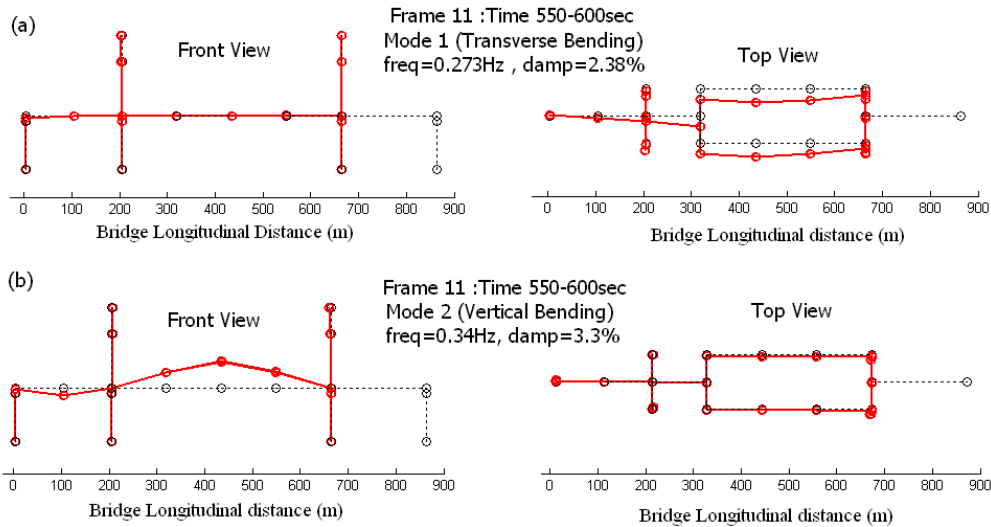


**Figure 9.** Characteristics of mode shapes with weak transverse-vertical coupling during the end of main shock 14:47 (Frame 11,  $t=500-550s$ ): (a) girder first transverse mode and (b) girder first vertical mode

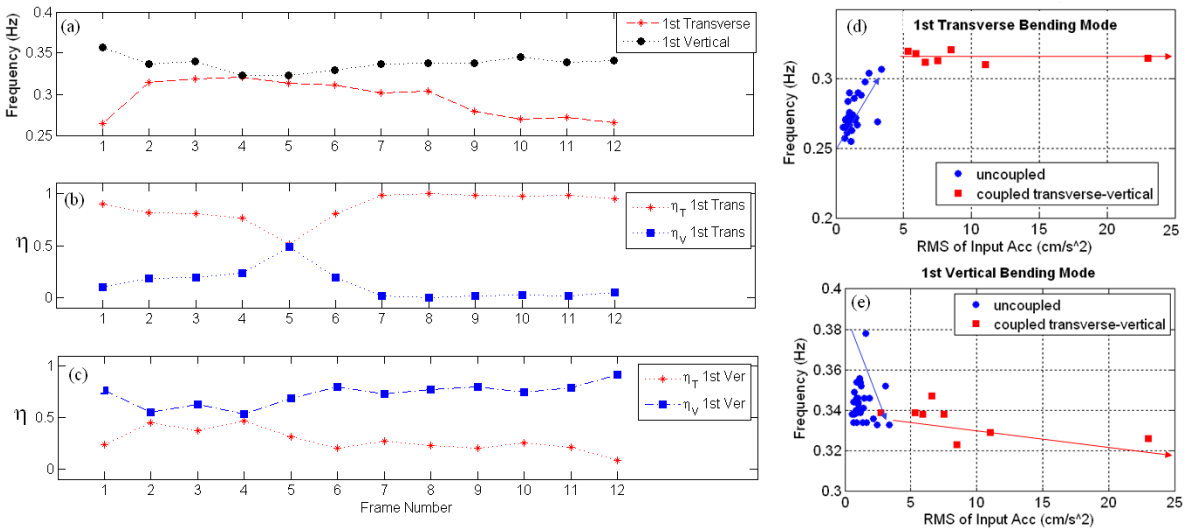


**Figure 10.** Main shock: (a) variation of natural frequency of the first transverse and first vertical bending for the main shock, (b) variation of coupling index  $\eta$  of the 1<sup>st</sup> transverse mode, (c) variation of coupling index  $\eta$  of the 1<sup>st</sup> vertical mode. Summary on variation of natural frequencies and transverse-vertical coupling of mode shapes with respect to input acceleration for main shock and nine aftershocks: (d) first transverse bending mode and (e) first vertical bending mode.

## 5. CONCLUSION AND RECOMMENDATION

Response analysis of the Yokohama Bay Bridge under the 2011 Great East Japan earthquake is discussed in this paper. During the main shock the bridge experienced intense shaking for about 10 minutes, but no structural damage was reported. Based on response analysis and system identification, the following conclusions can be drawn. (1) The input excitations recorded on the bridge foundation are still below the design and seismic-retrofit ground motions. (2) The bridge response during main shock was dominated by transverse movement of girder and tower. (3) During the main shock and aftershock March 15:16, girder accelerations show indication of response non-linearity as denoted by the time variation of natural frequencies and the change in transverse-vertical coupling of the first transverse and vertical mode shapes. (4) Relative displacement response, characteristics of acceleration spectra and type of longitudinal mode at the pier-to-girder and tower-to-girder connections suggest that the link bearing have functioned as intended. (5) Recorded accelerations, results of system identification and visual inspection indicate that transverse pounding between girder and tower have occurred. Despite its occurrence, transverse pounding did not cause any structural damage at this earthquake. In the future, however, the effect of transverse pounding on bridge should be investigated in more detail and countermeasure if necessary must be taken, in anticipation for larger earthquake excitation.



**Figure 11.** Circular scratch marks on the surface of wind shoe as a result of side bearing movement indicates girder longitudinal movement of about 8cm. (b) Location of head of tower link (P2) bottom head is connected to girder, top head is connected to tower. (c) Scratch marks on the surface of the bottom link head caused by combination of vertical and transverse movement of the girder. The arrows point to locations of three broken bolts caused by the movement.

## ACKNOWLEDGEMENT

We gratefully acknowledge Metropolitan Expressway Co. Ltd especially Mr. Kenji Namikawa for the access given to the monitoring data and the post-earthquake bridge visual inspection. Opinions and findings on this paper are those of the authors and do not represent those of the Metropolitan Expressway Co. Ltd.

## REFERENCES

- Fujino, Y. Kikkawa, H. Namikawa, K. and Mizoguchi, T. (2005). Seismic Retrofit Design of Long-Span Bridges on Metropolitan Expressways in Tokyo, *Proc. the 6<sup>th</sup> International Bridge Engineering Conference, Transportation Research Board, Boston Mass, USA, CD-ROM*
- Siringoringo, D.M. and Fujino, Y. (2006), Observed dynamic performance of the Yokohama-Bay Bridge from system identification using seismic records. *Structural Control and Health Monitoring*; **13**,226-244
- Maeda, K. Otsuka, A. Takano, H. (1991), The design and construction of Yokohama Bay Bridge, *Cable-Stayed Bridges Recent Developments and their Futures, M.Ito et.al. (Editors)*. Elsevier Science Publisher B.V. 377-395.
- Siringoringo, D.M. and Fujino, Y. (2008), System identification applied to long-span cable-supported bridges using seismic records. *Earthquake Engineering & Structural Dynamics*, **37**, 361-386.
- The Yokohama Bay Bridge (1991), *Published by Metropolitan Expressway Public Corporation, Tokyo Japan*, (in Japanese) 164-172.